Available online at website: https://journal.bcrec.id/index.php/bcrec

Bulletin of Chemical Reaction Engineering & Catalysis, 19 (1) 2024, 69-78

Research Article

A Study of ZSM-5 Molecular Sieve Shaping for an Innovative Cyclohexene Hydration Process

Baohe Wang[1,2], Dianyi Jin[1,2], Zhaobang Zhang[1,2], Zihan Ai[1], Jing Zhu[1,2,*]

[1]Key Laboratory for Green Chemical Technology of Ministry of Education, R&D Center for Petrochemical Technology, Tianjin University, Tianjin 300072, China
[2]Collaborative Innovation Center of Chemical Science and Engineering, Tianjin University, Tianjin 300072, China.

Received: 23th December 2023; Revised: 17th January 2024; Accepted: 17th January 2024
Available online: 22nd January 2024; Published regularly: April 2024

Abstract

The development of the zeolite molecular sieves (ZSM-5) molding technique is essential for the cyclohexene hydration reaction distillation process in both industrial and research settings. The reactive distillation process can solve many of the drawbacks associated with the existing technique of manufacturing cyclohexanol via cyclohexene hydration, such as high catalyst digestibility, low conversion rate, and operational challenges. This study developed a series of molded ZSM-5 catalysts with various binder types and contents were constructed. The suggested pseudo-boehmite and hydroxypropyl methylcellulose were chosen as binders for extrusion molding of ZSM-5. The effects of binders on the strength reliability were investigated by strength tests and statistical analysis of the Weibull function. The effects of binders on the physical structure, acidity, and catalytic performance of ZSM-5 were investigated by X-ray diffraction, scanning electron microscopy, physical adsorption of N_2, and desorption of NH_3. The findings demonstrate that the addition of binder has no effect on ZSM-5's crystal structure. The experiment's results showed that the molded catalyst could be used for the hydration process with over 95% selectivity and a yield of 10.45% cyclohexanol.

Keywords: Cyclohexene hydration; Reactive distillation; ZSM-5; Catalyst molding

How to Cite: B. Wang, D. Jin, Z. Zhang, Z. Ai, J. Zhu (2024). A Study of ZSM-5 Molecular Sieve Shaping for an Innovative Cyclohexene Hydration Process. *Bulletin of Chemical Reaction Engineering & Catalysis*, 19 (1), 69-78 (doi: 10.9767/bcrec.20095)

Permalink/DOI: https://doi.org/10.9767/bcrec.20095

1. Introduction

Cyclohexanol is a highly sought-after medium-to-high boiling point organic compound [1] that is used extensively to produce adipic acid, adipic diamine [2], caprolactam [3,4], and other essential components that are utilized in the manufacturing of polymers like nylon 66 and nylon 6 [5]. As a result, numerous academics have studied the cyclohexanol manufacturing process and related catalysts in great detail [6]. Currently, phenol hydrogenation [7–9], cyclohexane oxidation [10,11], and cyclohexene hydration [12] are the three primary methods used to produce cyclohexanol. The oldest method, phenol hydrogenation, is being gradually phased out due to the high cost of raw materials and the majority of precious metal catalysts employed in this process. The cyclohexane oxidation process potentially poses safety concerns associated with the introduction of oxidizing agents, and the generation of an extensive array of by-products adversely affects the selectivity of the reaction. The cyclohexene hydration process was first developed by Asahi Kasei in Japan. It is the most promising method due to its clear advantages in terms of safety, product selectivity and cost [13–15].

Because of its superior catalytic activity and thermal stability, ZSM-5 molecular sieve has become the primary catalyst source for the

---

* Corresponding Author.
Email: cj_zhu1975@tju.edu.cn (J. Zhu);
Tel.: + 86 22 27406959. Fax: +86 22 27406591

commercial synthesis of cyclohexanol [16–18]. To be acceptable for use in industrial reactors, ZSM-5 molecular sieve catalysts must meet specific requirements for strength and shape, as well as strong abrasion resistance and hydrothermal stability. Due to synthesis technique limitations, conventional ZSM-5 molecular sieves are in powder form, making direct use in distillation columns challenging [19–21]. Therefore, ZSM-5 molecular sieve fractions as the active components must be manufactured into catalysts with certain shapes and strengths through the molding process before they can be employed in industrial applications [22–24]. Gao *et al.* used pseudo-boehmite as a binder in the molding of ZSM-5 and observed that the catalyst formed by wet extrusion with dilute nitric acid and a 30% binder content had good catalytic activity and stability [25]. The strength of the molded catalysts showed a significant incremental trend with decreasing the particle size of the original molecular sieve powder, according to Guan *et al.*'s use of SB powders from various manufacturers as binders for ZSM-5 extrusion molding. However, the pore structure and relative crystallinity did not change significantly [26]. Ren *et al.* discovered that the amount of strong acid in the generated Mo/ZSM-5 catalysts made with zinc oxide as the carrier reduced while the reduction capacity of Mo species increased in the catalytic methane anaerobic aromatization reaction [27]. Research indicates that the primary binder utilized in the ZSM-5 catalyst molding process is Pseudo-boehmite, followed by hydroxypropyl methylcellulose, silica sol, kaolin, *etc*. The catalyst's physical characteristics will vary depending on the kind and quantity of binder employed. Additionally, various additives must be added during the molding process in order to meet the various needs of the catalysts. For example, the catalyst's resistance to toxicity must be increased, new compounds must be formed from the active components, appropriate pore structure must be provided, mechanical strength and stability must be improved, and so on [28].

The slurry bed process is the foundation of conventional aqueous cyclohexene production. In this process, the reaction is strictly governed by kinetics and there is very little mutual solubility between cyclohexene and water. This leads to low one-way yields and a significant amount of raw material recycling, which raises the energy consumption of the production process. In industry, reactive distillation is frequently employed to overcome equilibrium constraints. Distillation can also be used on-site to use up reaction heat. The core of the reactive distillation process application is the search for acceptable molding solutions for ZSM-5 molecular sieves. It is therefore very important to conduct research on the molding catalysts of ZSM-5 molecular sieves, specifically the effect of binder on the physical and chemical properties of the molding catalysts and the activity of catalytic cyclohexene hydration reaction [29]. Through an analysis of the impact of binder addition on the structure, pore size distribution, and acidity of the ZSM-5 catalysts that were formed, as well as a comparison of the effects of various forming techniques on the catalysts' catalytic performance, the best possible forming scheme was identified. This can serve as a foundation for future industrial applications.

2. Materials and Methods

2.1 Materials

ZSM-5 molecular sieve (produced by Henan Shenma Chemical Group); Pseudo-boehmite (99.9%, Shandong Zhanqi New Materials Co., Ltd.); Hydroxypropyl methylcellulose (99.9%, Tianjin Xiensi Opte Technology Co., Ltd.); Nitric acid (concentration 65-68%, analytical grade, Tianjin Jiangtian Chemical Technology Co., Ltd.); Sesbania Gum (99.9%, Henan Melo Industrial Co., Ltd.).

2.2 Catalysts Preparation

After thoroughly mixing the original molecular sieve powder and binder (pseudo-boehmite, hydroxypropyl methylcellulose) for ten minutes at room temperature, a specific mass of deionized water, sesbania gum, and nitric acid were added, and the mixture was kneaded for five to ten minutes to form a wet mass. The molded catalyst was then broken after 8 h of room temperature drying after the wet mass was put in a single-screw extruder and extruded through a customized die at a constant rotating speed of 60 rpm. For five hours, the catalyst was calcined in a muffle furnace at a rate of 2 °C per minute from ambient temperature to 550 °C. The last folding catalyst had a 2.1 mm diameter and a 3-5 mm length. It was cylindrical in shape. The suggested thin alumina and carboxymethylcellulose were used together as the binder with a mass ratio of 1:1 to prepare the folding catalysts with various binder contents and types. The contents of each component and the nomenclature of the catalysts are shown in Table 1. We called the unformed catalyst ZSM-5.

2.3 Catalyst Characterization

The catalyst mechanical strength was tested by quasi-static, single-particle pressure test. KQ-3 automatic strength tester was used to determine the mechanical strength of ZSM-5 molding body, the range of the instrument was 0-300 N, and the precision was 0.1 N. X-ray diffraction (XRD) phase analysis was carried out on a D/max-Ultimacies X-ray powder diffractometer (Japan Ricoh RIGAKU). Main technical indicators: Goniometric accuracy: ≤±0.02°; 2θ range: -10°~ +145°.

Fourier transform infrared (FT-IR) spectra characterization was carried out on a U.S. Thermos Scientific Nicolet iS20. The samples and potassium bromide powder were mixed and ground as the mass ratio of 1:200, and then the spectra were scanning at room temperature after forming by pressing. Main technical indicators: resolution 0.16 cm^{-1}, scanning range 400~4000 cm^{-1}.

The catalysts' morphology was determined by a JSM-7001F thermal field emission scanning electron microscope (SEM) with a voltage of 10 kV (JEOL, Akishima, Tokyo, Japan). SEM was used to directly observe the morphological characteristics of the product particles and the product particle size. The molecular sieve samples were sprayed with gold before observation.

Ammonia programmed thermal desorption (NH_3-TPD) was carried out on a Japan Microtrac BELCat II. It was used to determine the acid amount and acid intensity distribution of HZSM-5 molecular sieves under the following experimental conditions: 0.05 g of the sample was loaded into a quartz tube, and a carrier gas was passed through the tube, and the temperature was programmed to rise to 550 °C (the temperature increase rate was 10 °C/min), and the temperature was maintained at a constant level for 30 min, and then it was lowered to 150 °C, and the adsorption of NH_3 was carried out until saturated, then programmed thermal desorption was performed, and the sample was detected by TCD.

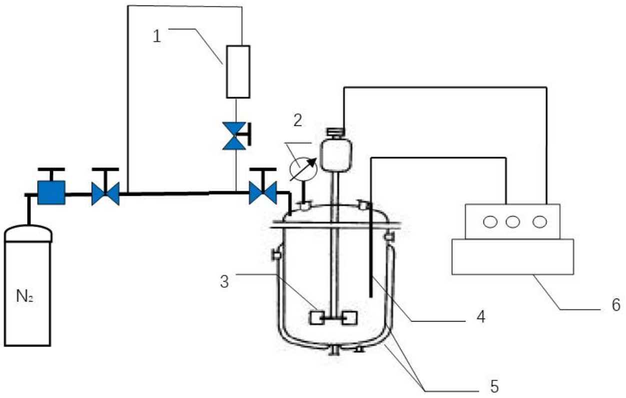

Figure 1. The reaction device of cyclohexene hydration. (1) Charging tank; (2) Manometer; (3) Agitator; (4) Thermoelectric couple; (5) Autoclave; (6) controller.

Low-temperature N_2 adsorption and desorption isotherms at 77 K were recorded using a Micromeritics ASAP 2010 instrument (Micromeritics, America). Before the measurements the samples were heated to 570 K in a vacuum for at least 12 h. The specific surface area, mesopore size pore distribution and micropore volume were calculated by the Braeuer–Emmett–Teller (BET) method, the Barrett–Joyner–Halenda (BJH) method and the t-plot method by Harkins and Jura (DeBoer) thickness equation, with a thickness range of 3.5 to 5 Å, respectively.

2.4 Catalyst Evaluation

The catalyst was evaluated in a 500 mL high pressure reactor, the reaction device is shown in Figure 1, 30 g of dry base catalyst was accurately weighed, 130 mL of deionized water was weighed and transferred to the reactor, mixed well and sealed. Nitrogen was replaced three times, the kettle pressure was increased to 0.75 MPa, and the stirring speed was 1000 rpm to start the temperature rise. After the kettle temperature rose to 125 °C, 100 mL of cyclohexene was pressed into the reaction kettle through the feed tank, and the timer was started. After the reaction for 2 h, the reaction kettle was cooled in ice water bath, and the temperature of the liquid in the reaction kettle was brought to room temperature, then the liquid was exported and the upper layer of oil was

Table 1. Catalyst formulation and naming.

Name of catalyst	Type of binder	Amount of binder (g)	Amount of ZSM-5 (g)	Amount of deionized water (g)	Amount of nitric acid (g)	Amount of Sesbania Gum (g)
ZSM-5	-	-	100	0	0	0
Z(NI10)	Pseudo-boehmite	10	80	70	10	3
Z(NI20)	Pseudo-boehmite	20	90	70	10	3
Z (NI10, PMC10)	Pseudo-boehmite, Hydroxypropyl methylcellulose	20	80	70	10	3
Z(PMC10)	Hydroxypropyl methylcellulose	10	90	70	10	3
Z(PMC20)	Hydroxypropyl methylcellulose	20	80	70	10	3

analysed. A GC-9790 gas chromatograph (manufactured by Wenling Fuli Analytical Instruments Co., Ltd.) was used to analyze the conversion rate and selectivity of cyclohexene.

3. Results and Discussion

3.1 Mechanical Properties of Catalysts

Weibull statistics can be used to calculate the probability of catalyst particle strength failure at a specified loading, providing a theoretical solution for predicting the mechanical reliability of solid catalysts [30,31]. Figure 2(a) shows the Weibull coordinate plot of the strength data, where the data points are the measured strength values. The corresponding Weibull distribution curves are shown in Figure 2(b), and the mechanical strength data of different types of samples are shown in Table 2.

As can be seen from the table, the coefficients of determination, R^2, for the five samples are, in order, 0.977, 0.974, 0.989, 0.982, and 0.971. their values are close to 1, indicating that the mechanical strength of the ZSM-5 extruded strip folding body can obey the Weibull distribution well [32]. The higher the fracture load at a specific low failure probability, the higher the mechanical strength reliability of the pellet. For this purpose, the fracture loads at low failure probabilities (F1%, F5%, F10%) for each sample were calculated by the Weibull distribution equation. Different types of bonding agents had a significant effect on the mechanical properties of the extruded strip samples. Among them, Z(NI20) using proposed Pseudo-boehmite as binder with dosage ratio of 1:4 (mass ratio with ZSM-5 catalyst raw powder) has the highest strength after extruded strip folding [33,34].

The Figure 2(b) illustrates that, with a constant binder type, the mechanical strength of the catalyst is directly proportional to the amount of binder incorporated. When the binder content is the same, the mechanical strength of the catalyst with proposed Pseudo-boehmite as binder is significantly higher than that of the catalyst molded with carboxymethyl cellulose, and the mechanical strength of the mixed binder is in between. The catalytic strength of different binders was higher than 80 N/cm, which meets the basic requirements of industrial production.

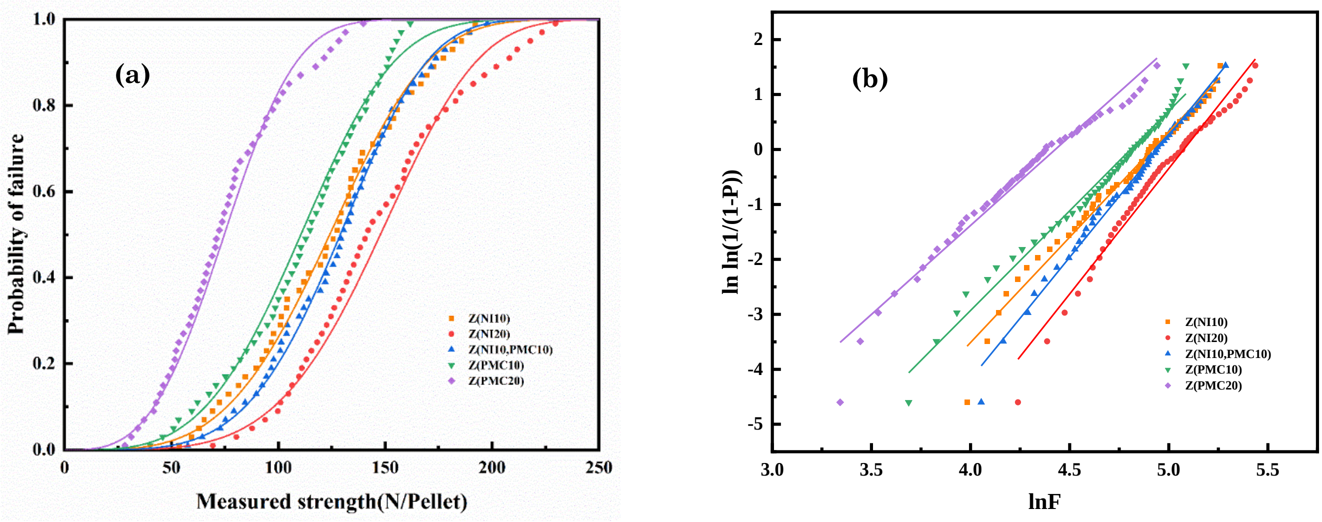

Figure 2. Weibull distribution curves (a) and Weibull plots (b) of the measured strength data of the extruded samples.

Table 2. Statistics of mechanical strength data for the extruded samples.

Sample	Mean (N)	Standard Deviation (N)	Weibull parameters			Fracture load with specific probability of failure (N)		
			M	F_0(N)	R^2	$F_{1\%}$	$F_{5\%}$	$F_{10\%}$
Z(NI10)	123.4	36.9	3.833	136.5	0.977	53.6	69.2	80.9
Z(NI20)	146.4	38.7	4.565	160.1	0.974	62.9	76.6	77.0
Z (NI10, PMC10)	127.8	33.4	4.432	140.1	0.989	57.6	72.9	79.2
Z(PMC10)	110.2	32.6	3.632	122.3	0.982	40.0	50.9	62.2
Z(PMC20)	75.2	27.7	3.236	83.7	0.971	28.3	34.3	42.9

3.2 Characterization of Catalysts

Figure 3 shows the XRD patterns for the prepared samples. It can be seen that the positions of the diffraction peaks of the corresponding multistage porous zeolite molecular sieves are basically the same when compared with the standard card, with five distinct characteristic diffraction peaks in the range of 2θ at 8-10° and 20-25° and no characteristic diffraction peaks of other crystalline phases, which proves that the powder samples are indeed the desired samples [35]. On the other hand, the crystalline structure is the same as that of the original powder sample, indicating that the introduction of the binder does not disrupt the MFI structure of ZSM-5 [36]. The intensity of the diffraction peaks of the moulded sample with the addition of binder was weakened, which was mainly due to the fact that the binder addition reduced the purity of the molding. Other than that, the dilute nitric acid introduced during the molding process did not significantly damage the crystal structure of ZSM-5 zeolite.

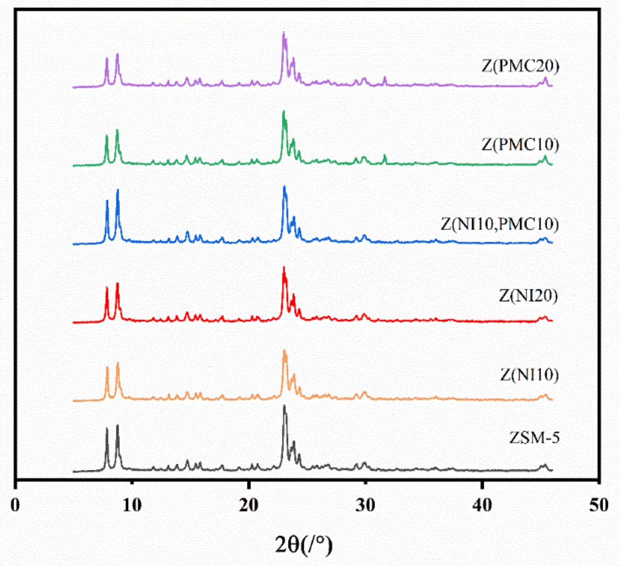

Figure 3. XRD patterns of the catalysts.

Figure 4 shows the SEM image of the powder sample and the SEM image of the extruded strip sample fractured after strength testing. It can be seen that the particles of the original powder sample are randomly dispersed and the spacing between the particles is large. After extrusion and folding, these particles are tightly bonded together due to the force, the distance between particles and particles is compressed, and the particles are bonded and cross-linked with each other. It can also be seen that the fracture surface of the molded sample is quite rough with many bumps and depressions.

The FT-IR spectrum of the catalyst is shown in Figure 5. The absorption peaks at 795 cm^{-1} (in-plane symmetric stretching vibration) and 455 cm^{-1} (bond-bending vibration) are typical of high silica materials, and the skeleton vibration peak at 550 cm^{-1} is attributed to the unique double five-membered ring structure of the MFI-type molecular sieves [37]. The catalyst has the characteristic FT-IR peaks of ZSM-5 zeolite, indicating that the synthesized sample has MFI structure [38].

As can be seen from the Figure 6, The NH$_3$-TPD curve of ZSM-5 generally has two absorption peaks, indicating that two different acidic sites

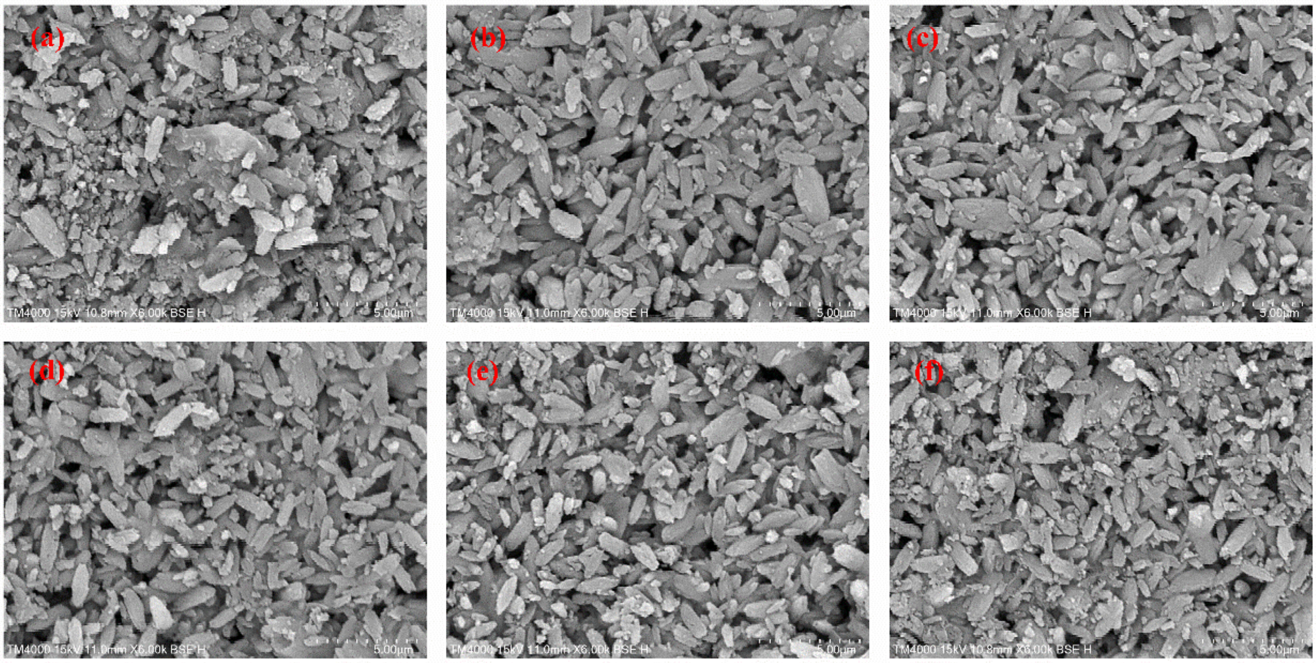

Figure 4. SEM images of the catalysts: (a) ZSM-5; (b) Z(NI10); (c) Z(NI20); (d) Z (NI10, PMC10); (e) Z(PMC10); (f) Z(PMC20).

may exist in this molecular sieve. The part located in the high-temperature region represents a strong acidic site, and on the contrary the one in the low-temperature region represents a weak acidic site. The absorption peaks in the high-temperature region are generally believed to be caused by strong Bronsted acids and Lewis acids, which come from the inner and outer skeleton Al [39], respectively, and these strong Bronsted acids and Lewis acids also play a major catalytic role in the hydration reaction of cyclohexene [40]. The absorption peaks in the low-temperature region are caused by weak Lewis acids, which are mainly from the external skeleton Al, such as Al $(OH)^{2+}$ and Al $(OH)^{2+}$, and a small portion from the internal skeleton Al [41].

The amount of acid possessed by the molecular sieves was derived by calculating the absorption peak area and is listed in Table 3. From the table, it can be seen that although the molded molecular sieves do not differ much in weak acid content, the amount of strong acid is drastically reduced, especially in the case of molded catalysts when hydroxypropyl methylcellulose is used as the binder. After the introduction of the binder, the position of the detachment peaks of the weak acid centres basically did not change, and the detachment peaks of the strong acid centres all moved toward the low temperature direction, indicating that the strength of the strong acid centres gradually decreased. This is due to the fact that since the binder contains aluminium, it may enter the ZSM-5 molecular sieve skeleton during the roasting process, lowering its silica-aluminium ratio and changing the catalyst acid properties.

The N_2 adsorption/desorption isotherms of all the molded catalysts and the catalyst raw powders showed typical type IV curves and H1 hysteresis loops (Figure 7), and this shape of the curves is usually caused by capillary condensation of mesopores at higher relative pressure valence, indicating that there are both micropores and mesopores in the structure of the molded ZSM-5 [42]. As compared to the ZSM-5 raw powder, Table 4 shows that the molded catalyst with the suggested thin pseudo-boehmite as binder has a higher pore volume and a lower specific surface area. It demonstrates that the addition of pseudo-boehmite causes ZSM-5's pores to get clogged,

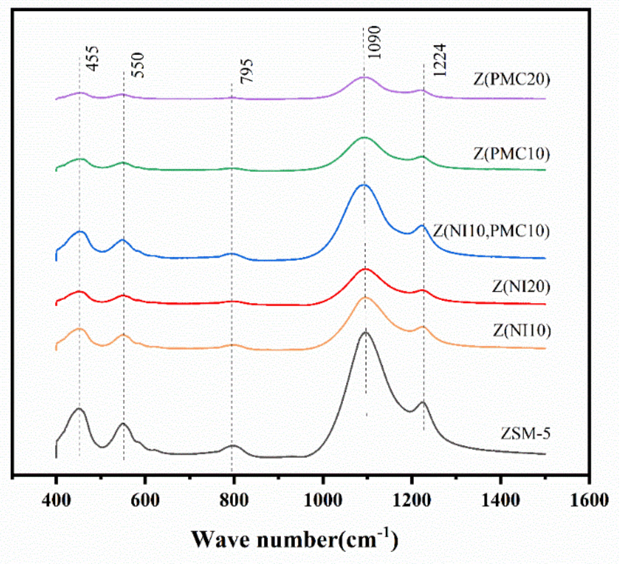

Figure 5. FT-IR spectra of the catalysts' structure.

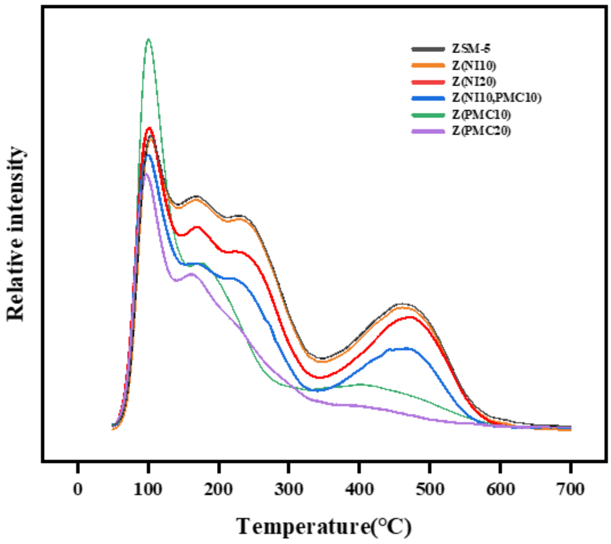

Figure 6. NH_3-TPD spectra of the catalysts.

Table 3. The amount of acid sites of prepared samples calculated from NH_3-TPD.

Sample	NH_3 adsorbed (mmol/g)		
	W[a]	S[b]	W+S[c]
ZSM-5	0.540	0.213	0.753
Z(NI10)	0.492	0.188	0.680
Z(NI20)	0.456	0.158	0.614
Z (NI10, PMC10)	0.464	0.110	0.574
Z(PMC10)	0.397	0.028	0.425
Z(PMC20)	0.386	0.013	0399

a: the weak acid content; b: the strong acid content; c: the total acid content.

reducing the material's specific surface area. Nevertheless, following roasting, the extrusion-molded catalyst will create mesopores between the binder and catalyst, which somewhat expands the pore volume. The decrease in specific surface area and pore volume of the catalyst with hydroxypropyl methylcellulose as binder may be due to the collapse of the skeleton caused by the action of the binder.

3.3 Catalytic Performance in Hydration of Cyclohexene

Catalytic activity tests for the hydration of cyclohexene were conducted on batch reactor equipment using formed ZSM-5 catalysts in different batches. The hydration of cyclohexene, an addition reaction, often involves side reactions such as isomerization or polymerization. The side products formed during synthesis vary with different catalysts. Due to the relatively small pores of the HZSM-5 molecular sieve, it is challenging for larger by-products, like 2-cyclohexenyl cyclohexanone, to form, and even when they do, they have difficulty diffusing out of the molecular sieve's channels. This leads to high selectivity for cyclohexanol during the reaction, typically exceeding 99%. Therefore, we use the conversion rate of cyclohexene as an evaluation indicator of the catalyst's effectiveness.

The catalyst activity of raw powder sieving is the best among the different binders, as Figure 8 illustrates. The relationship between the catalyst activity of catalyst folding binder type is as follows: raw powder crushing and sieving > extrusion folding with proposed thin pseudo-boehmite as the binder > extrusion folding with hydroxypropyl methylcellulose as the binder > extrusion folding with mixed binder, where the higher the catalytic activity, the lower the content of the catalyst binder. Cyclohexene conversion rate fell once the binder was introduced. This might be attributed to the binder's weakly basic character, which could lower the strength of the molecular sieve's acidic active sites during the formation process. The NH_3-TPD graphic shows a decline in the strength of strong acid sites following formation. Because cyclohexene hydration is largely catalyzed by Brønsted acids, the resulting catalyst has lower catalytic activity. Furthermore, according to the analysis of BET results, the introduction of the binder leads to blockage of microporous channels and a decrease in the specific surface area of the catalyst.

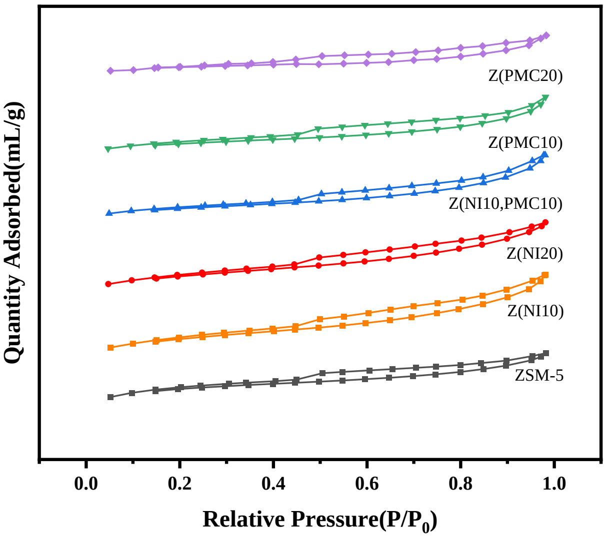

Figure 7. The low-temperature N_2 adsorption and desorption isotherms of the catalysts.

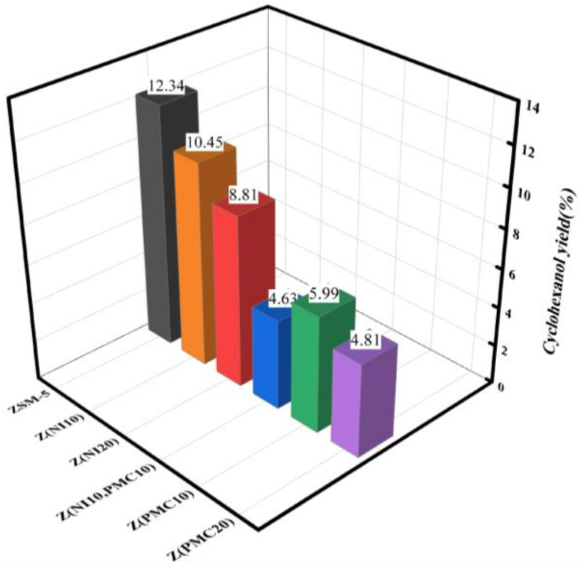

Figure 8. Cyclohexanol yields with different catalysts.

Table 4. Pore structure parameters of catalysts.

Sample	Specific Surface Area (m^2/g)	Pore Volume (cm^3/g)	Pore Diameter (nm)
ZSM-5	412	0.122	1.425
Z(NI10)	374	0.165	3.811
Z(NI20)	382	0.142	3.793
Z (NI10, PMC10)	356	0.115	3.812
Z(PMC10)	327	0.131	3.852
Z(PMC20)	313	0.126	3.641

In conclusion, the ZSM-5 raw powder catalyst produced the most cyclohexanol (12.34%), and its exposed surface area was larger. However, because it was not blended precisely, it was readily crushed and had a very low catalyst strength. However, since it has not undergone a strict forming process, the catalyst is extremely weak in strength and prone to powdering, making it challenging to apply directly in industrial reaction distillation processes. The formed catalyst using pseudo-boehmite as a binder demonstrates good catalytic activity, with a cyclohexene conversion rate of 10.45%, suggesting its suitability as a binder in the forming process of ZSM-5 molecular sieves.

In this experiment, the original powder ZSM-5 catalyst had a large exposed surface area, resulting in a high cyclohexanol yield of about 12.34%, which is comparable to current laboratory research results as shown in Table 5 [17]. However, due to its lack of undergoing a strict forming process, the catalyst is extremely weak and prone to powdering, making it difficult to apply directly in industrial reaction distillation processes. The catalyst formed using pseudo-boehmite as a binder showed good catalytic activity, with a cyclohexene yield of 10.45%. Although the yield of cyclohexene decreased, its mechanical strength meets industrial application standards, making it a recommended catalyst for the cyclohexene hydration reaction in distillation processes.

4. Conclusion

The effects of different binder types and contents on the mechanical properties, physical structure properties, acidity, and cyclohexene hydration reaction properties of the formed catalysts were investigated in this thesis, and the following conclusions were primarily obtained. The strength of the catalyst complies with the essential requirements for industrial production. The binding and aggregation of the binder with the molecular sieve grains resulted in a reduction in the specific surface area and pore volume of the molding catalyst micropores. When hydroxypropyl methylcellulose was utilized as the molding binder, the drop was evident, but it was little when the suggested thin pseudo-boehmite was employed as the binder. Forming with various binders had a minor influence on the Lewis acid distribution of the catalysts but a significant effect on the Bronsted acid distribution; with the addition of the binder, the strong acid center progressively shifted into the low temperature area. The shaped molecular sieves had lower Bronsted acid and Lewis acid quantities than unshaped molecular sieves, with the Bronsted acid amount decreasing the least when the suggested Pseudo-boehmite binder was utilized. In conclusion, using the suggested pseudo-boehmite as the binder allows the forming catalyst with the greatest and most stable mechanical strength to retain strong cyclohexene hydration reactivity. The experimental results form an important foundation for the commercial scale-up preparation of cyclohexene hydration catalyst.

Acknowledgments

This research was supported by Key Laboratory for Green Chemical Technology of Ministry of Education, R&D Center for Petrochemical Technology in China.

CRediT Author Statement

Baohe Wang: Conceptualization, Methodology, Investigation, Resources; *Dianyi Jin*: Data Curation, Writing, Review and Editing; *Zhaobang Zhang*: Data Curation, Writting Draft Preparation, Supervision; *Zihan Ai*: Writting Draft Preparation; *Jing Zhu*: Review and Data Curation. All authors have read and agreed to the published version of the manuscript.

References

[1] Sommer, T., Zapletal, M., Trejbal, J. (2018). Production of cyclic alcohols. *Chemical Papers*, 72 (10), 2397-2412. DOI: 10.1007/s11696-018-0508-5.

[2] Bart, J.C.J., Cavallaro, S. (2015). Transiting from Adipic Acid to Bioadipic Acid. Part II. Biosynthetic Pathways. *Industrial & Engineering Chemistry Research*, 54(2), 567-576. DOI: 10.1021/ie502074d.

[3] Wang, H., Qin, M., Wu, Q., Cheng, D.-G., Meng, X., Wang, L., Xiao, F.-S. (2022). Zeolite Catalysts for Green Production of Caprolactam. *Industrial & Engineering Chemistry Research*, 62(5), 2217–2224. DOI: 10.1021/acs.iecr.2c01693.

Table 5. Reaction conditions and yield of cyclohexene hydration.

Catalyst	Reaction temperature (°C)	Reaction time (h)	Water-oil ratio	Cyclohexene yield (%)
ZSM-5	125	3	1.2	12.34
Z(NI10)	125	3	1.2	10.45
HZSM-5(28) [a]	120	7	2	13

a: The catalyst is derived from references.

[4] Kumar, R., Shah, S., Das, P.P., Bhabavanbhai, G.G., Al Fatesh, A., Chowdhury, B. (2019). An overview of caprolactam synthesis. *Catalysis Reviews-Science and Engineering*, 61(4), 516-594. DOI: 10.1080/01614940.2019.1650876.

[5] Zong, B., Sun, B., Cheng, S., Mu, X., Yang, K., Zhao, J., Zhang, X., Wu, W. (2017). Green Production Technology of the Monomer of Nylon-6: Caprolactam. *Engineering*, 3(3), 379-384. DOI: 10.1016/j.Eng.2017.03.003.

[6] Gong, J., Hou, S., Wang, Y., Ma, X. (2023). Progress in Processes and Catalysts for Dehydrogenation of Cyclohexanol to Cyclohexanone. *Transactions of Tianjin University*, 29(3), 196-208. DOI: 10.1007/s12209-023-00358-x.

[7] Ali, M.A., Abutaleb, A. (2022). An Updated Comprehensive Literature Review of Phenol Hydrogenation Studies. *Catalysis Letters*, 152 (5), 1555-1581. DOI: 10.1007/s10562-021-03714-5.

[8] Xue, G., Yin, L., Shao, S., Li, G. (2022). Recent progress on selective hydrogenation of phenol toward cyclohexanone or cyclohexanol. *Nanotechnology*, 33 (7), 072003. DOI: 10.1088/1361-6528/ac385f.

[9] Chen, H., Sun, J. (2021). Selective hydrogenation of phenol for cyclohexanone: A review. *Journal of Industrial and Engineering Chemistry*, 94, 78-91. DOI: 10.1016/j.jiec.2020.11.022.

[10] Dhakshinamoorthy, A., Lopez-Frances, A., Navalon, S., Garcia, H. (2022). Porous Metal Organic Frameworks as Multifunctional Catalysts for Cyclohexane Oxidation. *ChemCatChem*, 14 (22), e202201036. DOI: 10.1002/cctc.202201036.

[11] Perkel, A.L., Voronina, S.G. (2019). Liquid-phase oxidation of cyclohexane. Cyclohexyl hydroperoxide, cyclohexanol, and cyclohexanone, mechanisms of formation and transformation. *Russian Chemical Bulletin*, 68(3), 480-492. DOI: 10.1007/s11172-019-2443-1.

[12] Zheng, H., Lin, M., Qiu, T., Shen, Y., Tian, H., Zhao, S. (2017). Simulation study of direct hydration of cyclohexene to cyclohexanol using isophorone as cosolvent. *Chemical Engineering Research & Design*, 117, 346-354. DOI: 10.1016/j.cherd.2016.10.031.

[13] Liu, X., Luo, H., Lei, Y., Wu, X., Gani, R. (2022). Heat-pump-assisted reactive distillation for direct hydration of cyclohexene to cyclohexanol: a sustainable alternative. *Separation and Purification Technology*, 280, 119808. DOI: 10.1016/j.seppur.2021.119808.

[14] Taipabu, M.I., Novita, F.J., Lee, H.-Y., Handogo, R. (2021). Improvement of Cyclohexene/ Cyclohexane separation process design via chemical looping technology using reactive distillation and thermally coupled configurations. *Chemical Engineering and Processing-Process Intensification*, 168, 108587, Article. DOI: 10.1016/j.cep.2021.108587.

[15] Hu, M., Tian, H. (2021). Design of process and control scheme for cyclohexanol production from cyclohexene using reactive distillation. *Chinese Journal of Chemical Engineering*, 40, 96-105. DOI: 10.1016/j.cjche.2020.11.029.

[16] Tian, H., Liu, S., Liu, Q. (2022). HZSM-5 zeolite modification and catalytic reaction mechanism in the reaction of cyclohexene hydration. *RSC Advances*, 12 (38), 24654-24669. DOI: 10.1039/d2ra04285a.

[17] Spod, H., Lucas, M., Claus, P. (2017). Hydration of Cyclohexene into Cyclohexanol using H-ZSM5 as Catalyst. *Chemie Ingenieur Technik*, 89(6), 750-756. DOI: 10.1002/cite.201600160.

[18] Wang, S., Li, C., Wen, Y., Wei, H., Li, B., Wang, X. (2016). Microparticle HZSM-5 zeolite as highly active catalyst for the hydration of cyclohexene to cyclohexanol. *Research on Chemical Intermediates*, 42 (12), 8131-8142. DOI: 10.1007/s11164-016-2584-x.

[19] Gao, J., Li, X., Shi, D., Qu, L., Zhang, J. (2020). Honeycomb molding process of ZSM-5 molecular sieves and adsorption to toluene. *Modern Chemical Industry*, 40 (6), 123-127.

[20] Wang, J., Gao, X., Chen, G., Din, C. (2019). Forming pure shaped ZSM-5 zeolite bodies by a steam-assisted method and their application in methanol to aromatic reactions. *RSC Advances*, 9(49), 28451-28459. DOI: 10.1039/c9ra05513d.

[21] Xu, Y., Song, Y., Zhang, Z.-G. (2017). A binder-free fluidizable Mo/HZSM-5 catalyst for non-oxidative methane dehydroaromatization in a dual circulating fluidized bed reactor system. *Catalysis Today*, 279, 115-123. DOI: 10.1016/j.cattod.2016.03.037.

[22] Moon, S., Chae, H.-J., Park, M.B. (2019). Dehydration of Bioethanol to Ethylene over H-ZSM-5 Catalysts: A Scale-Up Study. *Catalysts*, 9(2), 186. DOI: 10.3390/catal9020186.

[23] Li, S., Xia, L., Li, J., Liu, X., Sun, J., Chi, Y., Wang, H., Li, C., Song, Y. (2019). Effect of forming conditions on the performance of catalytic decomposition of N_2O over Co/ZSM-5 catalyst. *Chemical Industry and Engineering Progress*, 38(4), 1746-1752.

[24] Jia, C., Zong, L., Wen, Y., Xu, H., Wei, H., Wang, X. (2019). Synthesis and scale-up of ZSM-5 aggregates with hierarchical structure. *Research on Chemical Intermediates*, 45 (7), 3913-3927. DOI: 10.1007/s11164-019-03828-x.

[25] Gao, J., Zhou, H., Zhang, F., Ji, K., Liu, P., Liu, Z., Zhang, K. (2022). Effect of Preparation Method on the Catalytic Performance of HZSM-5 Zeolite Catalysts in the MTH Reaction. *Materials*, 15 (6), 2206. DOI: 10.3390/ma15062206.

[26] Guan, C., Wang, L., Qi, J., Song, C., Zhang, W., Yong, X., Zhang, A., Jin, Z. (2019). Influence of shaping condition on properties of ZSM-5 catalyst. *Applied Chemical Industry*, 48(8), 1850-1854.

[27] Ren, D., Sai, F., Zhao, Y., Xia, Y., Bao, D., Wang, X. (2017). Methane dehydroaromatization in the absence of oxygen over extruded Mo/ZSM-5 with Al_2O_3-ZnO. *Chemical Research and Application*, 29 (10), 1492-1497. DOI: 10.3724/SP.J.1088.2010.90939

[28] Xu, Y., Wang, D., Li, Q., Zhang, D., Li, M., Hou, K. (2016). Influences of adhesives on structure and hydrothermal/mechanical stability of unsupported composite Mo-Ni oxide catalysts. *Petrochemical Technology*, 45 (2), 174-180.

[29] Li, N., Wang, Z., Zhang, B., Sun, H., Yang, W. (2016). Preparation and Catalytic Performance of Binder-Free MCM-22 Catalyst. *Chemical Reaction Engineering and Technology*, 32(3), 198-202.

[30] Zhang, L., Xu, A., An, L., Li, M. (2022). Bayesian Inference of System Reliability for Multicomponent Stress-Strength Model under Marshall-Olkin Weibull Distribution. *Systems*, 10(6), 196. DOI: 10.3390/systems10060196.

[31] Liao, D., Zhu, S.-P., Keshtegar, B., Qian, G., Wang, Q. (2020). Probabilistic framework for fatigue life assessment of notched components under size effects. *International Journal of Mechanical Sciences*, 181, 105685. DOI: 10.1016/j.ijmecsci.2020.105685.

[32] Zhang, H., Jiang, T., Yaseen, H.A.S.M., Zhao, Y., Wang, S., Ma, X. (2021). Pelletization and attrition of CaO-based adsorbent for CO2 capture. *Asia-Pacific Journal of Chemical Engineering*, 16(4), e2656. DOI: 10.1002/apj.2656.

[33] Xu, D., Ding, C., Li, F., Liu, Y., He, M. (2023). P-Modified Deactivated TS-1 as an Efficient Catalyst for Catalytic Cracking of Pentene to Ethene and Propene. *Chemical Journal of Chinese Universities*, 44(8), 20230094. DOI: 10.7503/cjcu20230094.

[34] Wang, Z., Ma, A., Yu, Z., Liu, H., Wang, J., Liu, J., Zhang, X., Zhang, R. (2022). Development And Application of Rf-4catalyst for Moving-Bed Light Hydrocarbon Aromatization. *Petroleum Processing and Petrochemicals*, 53(2), 46-52.

[35] Liang, T., Chen, J., Qin, Z., Li, J., Wang, P., Wang, S., Wang, G., Dong, M., Fan, W., Wang, J. (2016). Conversion of Methanol to Olefins over H-ZSM-5 Zeolite: Reaction Pathway Is Related to the Framework Aluminum Siting. *ACS Catalysis*, 6 (11), 7311-7325. DOI: 10.1021/acscatal.6b01771.

[36] Xiong, H., Liu, Z., Chen, X., Wang, H., Qian, W., Zhang, C., Zheng, A., Wei, F. (2022). In situ imaging of the sorption-induced subcell topological flexibility of a rigid zeolite framework. *Science*, 376 (6592), 491-496. DOI: 10.1126/science.abn7667.

[37] Nishu; N., Liu, R., Rahman, M.M., Sarker, M., Chai, M., Li, C., Cai, J. (2020). A review on the catalytic pyrolysis of biomass for the bio-oil production with ZSM-5: Focus on structure. *Fuel Processing Technology*, 199, 106301. DOI: 10.1016/j.fuproc.2019.106301.

[38] Mueller, S., Liu, Y., Vishnuvarthan, M., Sun, X., van Veen, A.C., Haller, G.L., Sanchez-Sanchez, M., Lercher, J.A. (2015). Coke formation and deactivation pathways on H-ZSM-5 in the conversion of methanol to olefins. *Journal of Catalysis*, 325, 48-59. DOI: 10.1016/j.jcat.2015.02.013.

[39] Lee, H., Zones, S.I., Davis, M.E. (2003). A combustion-free methodology for synthesizing zeolites and zeolite-like materials. *Nature*, 425(6956), 385-388. DOI: 10.1038/nature01980.

[40] Jin, R., Ma, K., Xu, S., Wei, Y., Song, L., Li, Z., Zhang, P., Wang, Y., Wang, J., Zhang, Z., Ma, X., Hu, H., Dai, C., Guo, X. (2022). Effect of acid distribution and pore structure of ZSM-5 on catalytic performance. *Reaction Chemistry & Engineering*, 7 (10), 2152-2162. DOI: 10.1039/d2re00065b.

[41] Lónyi, F., Valyon, J. (2001). On the interpretation of the NH3-TPD patterns of H-ZSM-5 and H-mordenite. *Microporous and Mesoporous Materials*, 47 (2-3), 293-301. DOI: 10.1016/s1387-1811(01)00389-4.

[42] Silva, B.J.B., Sousa, L.V., Sarmento, L.R.A., Carvalho, R.P., Quintel, P.H.L., Pacheco, J.G.A., Frety, R., Silva, A.O.S. (2019). Effect of desilication on the textural properties, acidity and catalytic activity of zeolite ZSM-23 synthesized with different structure-directing agents. *Microporous and Mesoporous Materials*, 290, 109647. DOI: 10.1016/j.micromeso.2019.109647.